Applied Catalysis B: Environmental 91 (2009) 489–498

Contents lists available at ScienceDirect

Applied Catalysis B: Environmental

journal homepage: www.elsevier.com/locate/apcatb

Soot combustion over silver-supported catalysts

Eleonora Aneggi [a,*], Jordi Llorca [b], Carla de Leitenburg [a], Giuliano Dolcetti [a], Alessandro Trovarelli [a]

[a] Dipartimento di Scienze e Tecnologie Chimiche, Università di Udine, Udine, via cotonificio 108, 33100 Udine, Italy
[b] Institut de Tècniques Energètiques, Universitat Politècnica de Catalunya, Diagonal 647, 08028 Barcelona, Spain

ARTICLE INFO

Article history:
Received 17 April 2009
Received in revised form 15 June 2009
Accepted 18 June 2009
Available online 24 June 2009

Keywords:
Ceria
CeO_2
Zirconia
ZrO_2
Alumina
Al_2O_3
Silver
Ag
Ag_2O
Oxygen storage
Soot oxidation
Diesel
Combustion

ABSTRACT

In this study the characterization and soot oxidation activity of Ag-based catalysts deposited on alumina, ceria and zirconia have been investigated. The combustion of soot was shown to be promoted by the presence of silver, especially in a zero valent state, over all the supports investigated. Presence of silver in a positive oxidation state is favoured with CeO_2, while zero valent silver dominates over alumina and zirconia. This is likely attributed to the oxygen storage capacity of ceria which stabilizes silver in an oxidized form. Soot oxidation starts at low temperature (around 500 K for Ag on ZrO_2) with a T_{50} in the range of 600–640 K. Deactivation under strong ageing conditions (1023 K for 12 h) is negligible with alumina and zirconia, while in the presence of ceria, which slows down formation of metallic silver from Ag_2O, loss of activity following thermal treatments at high temperatures becomes more intense.

1. Introduction

It is widely recognized that diesel engine vehicles are fated to significantly increase their worldwide penetration, even in countries where the present market share is not remarkable as that of gasoline engines. Exhaust abatement in diesel engines poses a series of challenges to meet new legislation especially for NO_x and particulate reduction [1–3]. The severity of regulation requires solutions based on de-NO_x systems and catalytic traps for either light and heavy duty engines.

The most effective and widely applied after-treatment technology for the particulate matter (PM) control is based on diesel particulate filter (DPF) [4–6]. These devices perform the filtration of exhaust gases by removing a significant fraction of particulate, which adheres to the filter walls; they must be periodically regenerated to remove the entrapped soot and avoid increase of pressure drop at the exhaust.

The regeneration process can be carried out by combustion of PM by injection of extra fuel; this, however, implies an extra fuel consumption, which reduces the engine efficiency; moreover, excessive heating can damage both filter and the other after-treatment devices (i.e. the de-NO_x catalysts). Therefore remarkable research efforts have been made to find alternative solution for filter regeneration at lower temperature.

In one approach, a catalyst is deposited on the filter media which allows regeneration to occur in a continuous or periodic manner, during the regular operation of the system [1]. The main purpose of the catalyst is therefore to facilitate a passive regeneration of the filter by enabling the oxidation of diesel PM under exhaust temperatures reached during regular operation of the engine/vehicle, typically in the 573–673 K range. In the absence of the catalyst, particulates can be oxidized at appreciable rates only at temperatures around 800–900 K, which can occur only at full load conditions. Catalytic approach is affected by several drawbacks: catalytic filter regeneration is very complex because of the very variable conditions of reaction; moreover, the process is quite slow because of the poor soot/catalyst contact. Another important operative constraint is represented by the wide range of temperature expected for the exhausted gases (from 473 to 873 K), depending upon engine load. Consequently a useful catalyst has to operate efficiently at low temperatures but has also to be thermally stable.

* Corresponding author.
E-mail address: eleonora.aneggi@uniud.it (E. Aneggi).

0926-3373/$ – see front matter © 2009 Elsevier B.V. All rights reserved.
doi:10.1016/j.apcatb.2009.06.019

Diverse catalytic materials have been studied in the last years based on different properties. One approach is to increase the contact points between the soot particle and the catalysts by using fuel borne catalyst additives or molten salt catalysts which can wet the soot surface and therefore decrease the oxidation temperature [7–9]. The use of a more powerful oxidant than oxygen, like NO_2, can also efficiently decrease the soot combustion temperature [10–12]. Among the several catalyst components used for soot oxidation the most promising formulations are based on addition of potassium to oxides of transition metals (such as Cu, V, Mo, Co or Fe) [8,9,13–17], or on systems based on combination of Co, K/MgO or Ba, K/CeO_2 [11,18,19], or on the use of perovskites like $La_{1-x}Cs_xCoO_3$, $LaMnO_3$, and $La_{0.9}K_{0.1}Cr_{0.9}O_{3-\gamma}$ [20]. Several supports like ZrO_2, TiO_2, Al_2O_3 and CeO_2 have also been reported for use in diesel soot oxidation. Ceria alone or in combination with other oxides is active in oxidation of carbon particles [11,12,21–33] and the mechanism of action is associated to the redox activity of the material; that is the effectiveness of the catalyst can be related to its ability to deliver oxygen from the lattice to the gas phase (or better to the soot reactant) in a wide temperature range. It has been reported that the use of supports based on cerium oxide confers interesting properties to soot combustion catalysts due to high availability of surface oxygen and high surface reducibility [24,25,32,33]. The success of oxygen storage systems based on ceria is due to their ability to change oxidation state during operation (i.e. CeO_2 to CeO_{2-x}) maintaining structural integrity, thus allowing oxygen uptake and release to occur easily. The use of CeO_2-supported metals can increase the benefit of bare ceria due to the establishment of an interaction between the metal and the support that enhances the redox characteristics of pure ceria [10,11,25,34,35]. In addition, a mechanism in which the redox of CeO_2 contributes to the generation of superoxide species in a more efficient manner compared to other oxides has been recently put forward to explain higher reactivity among a series of catalyst supports [36].

Silver is known to be an efficient partial oxidation catalyst and it is industrially used for epoxidation of ethylene to ethylene epoxide [37,38] and for oxi-dehydrogenation of methanol to formaldehyde [39–41]. Other applications in which Ag has shown remarkable performances include NO_x abatement [42,43], ammonia oxidation [44] and oxidation of methane, carbon monoxide and organic volatile compounds [45–47]. The use of Ag deposited on ceria was also found to increase the rate of carbon gasification compared to other noble metals [48] establishing a sort of enhanced metal–support interaction. Recently the potential of silver on alumina catalyst for the oxidation of carbon particle in the presence of NO_x and oxygen has been also reported [49].

These properties stimulated us to investigate in detail the behaviour of silver deposited on ceria in the oxidation of carbon soot particles. The study was also extended to other supports like alumina and zirconia, that were also reported to be effective in several oxidation reaction in the presence of Ag [38,40,42,44,49]. The aim is to obtain a better understanding of Ag/Ag-oxide chemistry and their interaction with the support as related to soot oxidation reaction. We have found that these catalytic materials are able to perform carbon oxidation at temperature as low as 600 K, as studied by temperature programmed oxidation and thermogravimetric methods. Structural details, monitored by HRTEM and XRD, allowed us to distinguish also the effect of different supports on the behaviour of supported Ag/Ag_2O particles.

2. Experimental procedures

2.1. Materials

Silver-doped catalysts (1–10 wt%) were prepared by incipient wetness impregnation of CeO_2, ZrO_2 and γ-Al_2O_3 (Grace Davison),

Table 1
Characteristics of samples used in this study.

Sample	Ag (wt%)	Surface area (m^2/g)	
		Fresh	Aged[a]
CeO_2	–	49	22
Ce1Ag	1	47	12
Ce5Ag	5	37	13
Ce10Ag	10	34	13
ZrO_2	–	59	27
Zr1Ag	1	48	20
Zr5Ag	5	45	19
Zr10Ag	10	39	16
Al_2O_3	–	180	159
Al1Ag	1	175	158
Al5Ag	5	165	157
Al10Ag	10	156	153

[a] After treatment under air at 1023 K for 12 h.

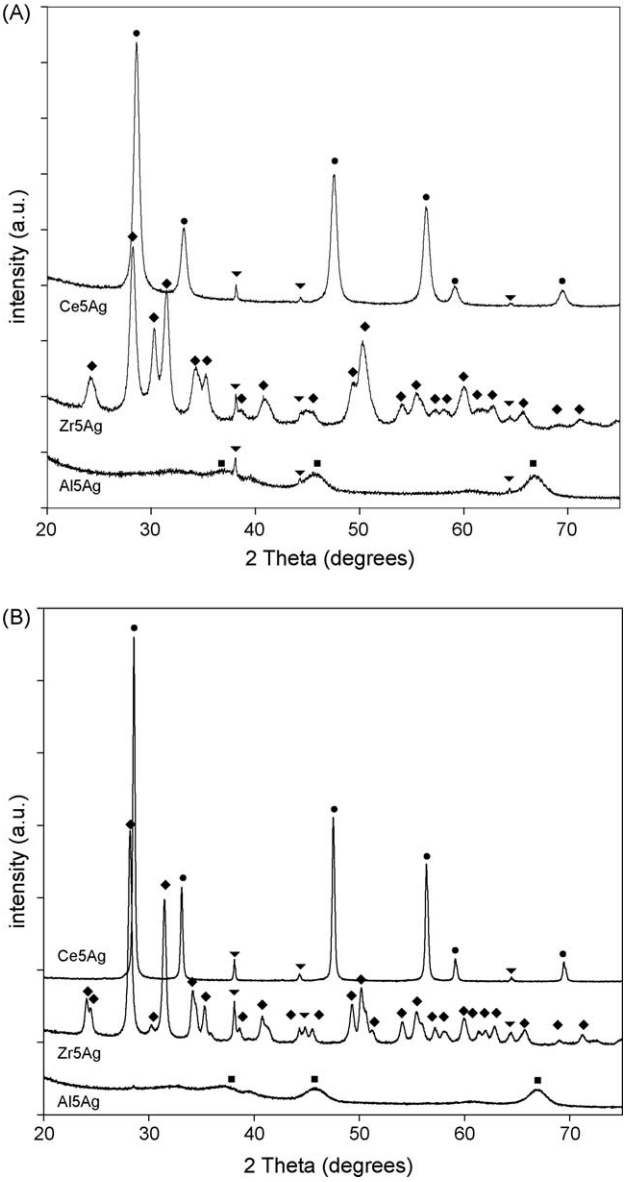

Fig. 1. XRD profiles of fresh (A) and aged (B) samples: Ag, ▼; CeO_2, ●; ZrO_2, ◆; Al_2O_3, ■.

with an aqueous solution (0.3–0.8 M) of the nitrate salt, $AgNO_3$ (Aldrich). They were dried at 373 K overnight and calcined in air at 773 K for 3 h (fresh samples) and at 1023 K for 12 h (aged samples). Ageing in the presence of water has been also carried out at 1023 K for 4 h under N_2/H_2O mixtures (10 vol% H_2O).

Textural characteristics were measured according to the B.E.T. method by nitrogen adsorption at 77 K, using a Tristar 3000 gas adsorption analyzer (Micromeritics). Structural features of the catalysts were investigated by X-ray diffraction. Diffractograms were recorded on a Philips X'Pert diffractometer (equipped with a real time multiple strip detector) operated at 40 kV and 40 mA using Ni-filtered Cu-Kα radiation. Spectra were collected using a step size of 0.02° and a counting time of 40 s per angular abscissa in the range 20–145°. The Philips X'Pert HighScore software was used for phase identification. In-situ XRD were also performed with a reaction chamber (XRK900, Anton Parr) that allows to perform studies under operative conditions.

For high-resolution transmission electron microscopy studies (HRTEM), a JEOL JEM 2010F electron microscope equipped with a field emission gun was used working at an accelerating voltage of 200 kV. Samples were dispersed in ethanol in an ultrasonic bath and a drop of supernatant suspension was poured onto a holey carbon coated grid and dried completely before measurements.

Redox behaviour was measured by temperature programmed reduction experiments (TPR) with a AutoChem II 2920 instrument (Micromeritics). Samples (50–60 mg) were heated from r.t. to 1073 K at a constant rate (10 K/min) in a U-shaped quartz reactor, under a flowing hydrogen/argon mixture (30 ml/min, 5.11% H_2 in Ar) while monitoring the hydrogen consumption.

2.2. Catalytic activity

Soot oxidation activity was tested by running TGA experiments (Q500, TA Instruments) and measuring the weight loss against temperature of catalyst/soot mixtures under flowing air [6,13,50–55]. A soot/catalyst weight ratio of 1:20 was used; each catalyst was accurately mixed with soot (Printex-U, Degussa AG) in a mortar for 10 min in order to achieve a tight contact [56]. This mixture (ca. 20 mg) was pretreated for 1 h at 423 K to eliminate traces of absorbed water, then it was heated at a constant rate (10 K/min) up to 1073 K. As a measure of activity we used the temperature at which 50% of weight loss is observed (T_{50}, corresponding to the temperature at which 50% of soot is

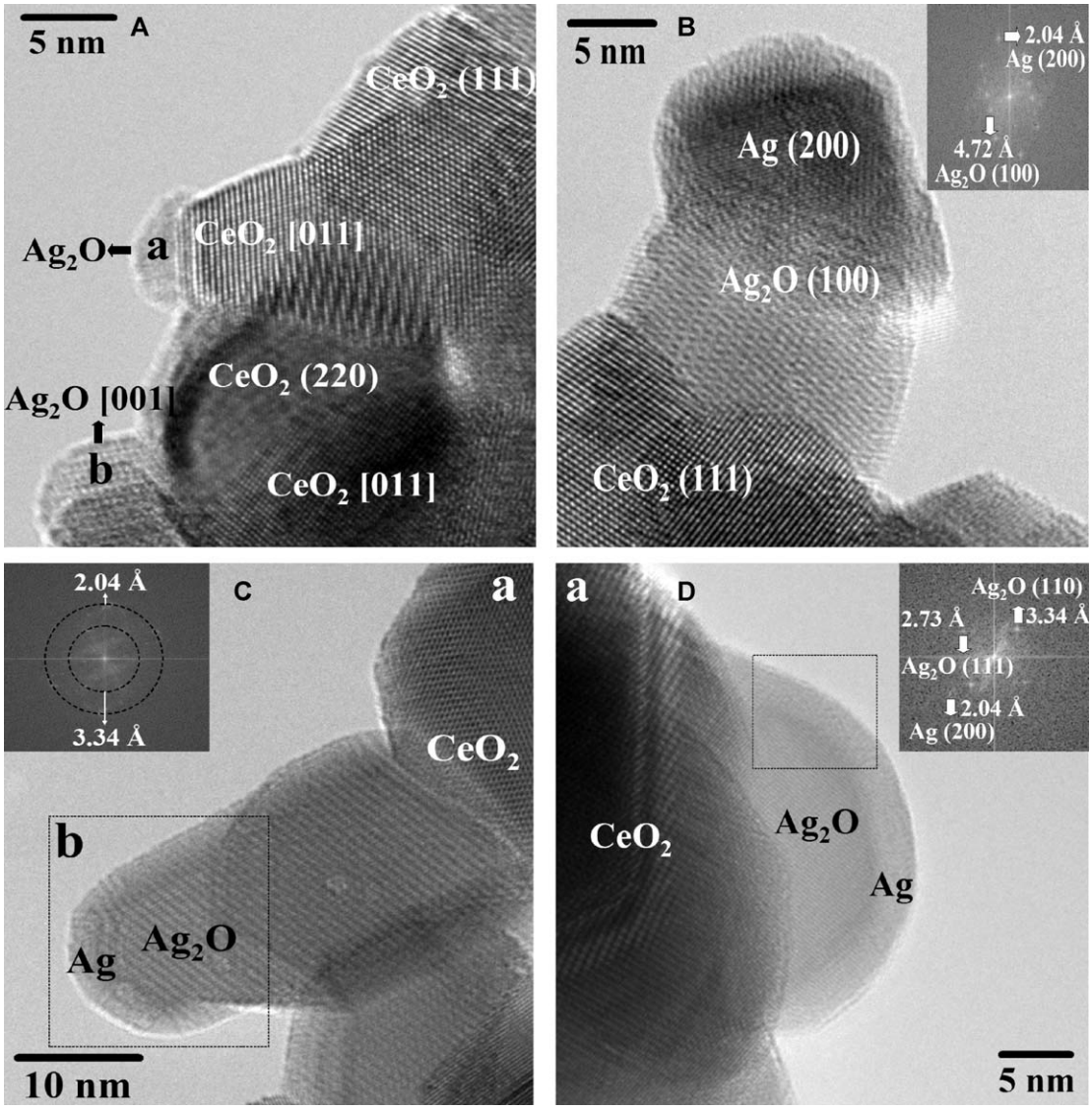

Fig. 2. HRTEM images of fresh (A and B) and aged (C and D) Ce5Ag.

converted under tight contact conditions). The kind of contact between catalyst and soot is extremely important [1,57]: the tight contact conditions are not fully representative of the real working conditions experienced by the catalyst deposited in a catalytic trap, but they allow a rapid screen of catalysts in reproducible experimental conditions. Reproducibility of results were tested by running several TG experiments on similar samples and the results in terms of T_{50} were always within ±3 K. A series of measurement were also carried out under loose contact conditions by mixing soot and catalyst with a spatula in order to work under more realistic conditions.

The catalytic activity for the combustion of soot [1,58–62] was also determined from peak-top temperature (T_m) during temperature programmed oxidation (TPO) of catalyst–soot mixtures. During the TPO measurements 25 mg of the above mixture were heated at a constant rate (10 K/min) in a quartz reactor, while the gas flow (N_2 with 6% of O_2) was kept fixed at 0.4 l/min. The catalyst temperature was checked by a chromel–alumel thermocouple, located on the catalyst bed. The outlet composition was measured by IR and paramagnetic gas analyzers (Magnos 106 and Uras14, ABB), by recording the percentages of CO, CO_2 and O_2 in the exhaust.

3. Results and discussion

3.1. Materials

Table 1 summarizes B.E.T. surface areas of the supports and silver-supported catalysts in a fresh state and after ageing. It can be seen that the addition of silver results in a drop in surface area at the loadings used in this study. This is typically observed upon addition to high surface area supports of oxides possessing high specific weight and low porosity [63,64] and the effect is more pronounced at high loadings. After treatment at 1023 K a significant drop in surface area is observed in CeO_2 and ZrO_2 either alone or with silver; this confirms that stability of the two supports is critical at these temperature [65] and that silver has no influence on their stability. With alumina the drop in surface area is less significant and in the presence of Ag, fresh and aged samples show similar surface area values.

The characteristics of each catalyst group (5 wt% composition was chosen as representative of each support), fresh and after ageing, were also studied by XRD, TG and HRTEM measurements. Fig. 1A and B shows the X-ray diffraction profiles of fresh and aged catalysts respectively. In the case of ceria, peaks belonging to the fluorite phase are clearly observed; in addition to those peaks the presence of signals at $2\theta = 38.1^\circ$, 44.3° and 64.5° indicates formation of metallic silver. Similarly, in Ag/ZrO_2 and Ag/Al_2O_3 samples, in addition to the peaks due to the support, signals due to metallic Ag are observed. In fresh Al5Ag the signals due to metallic silver are very weak and in the aged samples no signals are detectable indicating a well-dispersed phase. No evidence for the presence of Ag_2O crystallites was obtained from XRD profiles.

A more detailed morphological and structural analysis has been carried out on selected compositions by HRTEM. Ce5Ag sample calcined in air at 773 K for 3 h (fresh sample) contains well-dispersed silver particles corresponding to metallic Ag and Ag_2O. In the catalyst two types of particles are encountered: Ag_2O (around 5 nm in diameter) in contact with CeO_2 (Fig. 2A) and metallic Ag crystallites (Fig. 2B) in contact with larger Ag_2O particles (in the

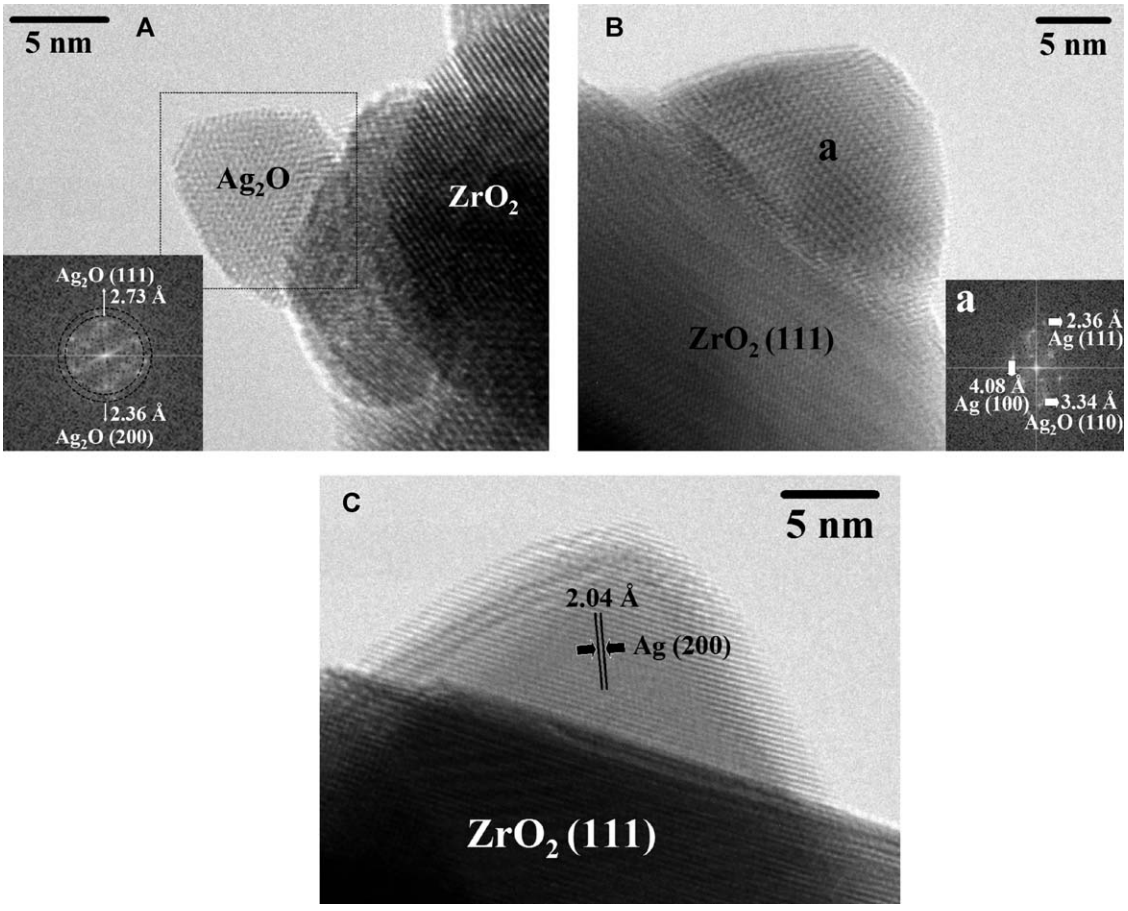

Fig. 3. HRTEM images of fresh (A) and aged (B and C) Zr5Ag.

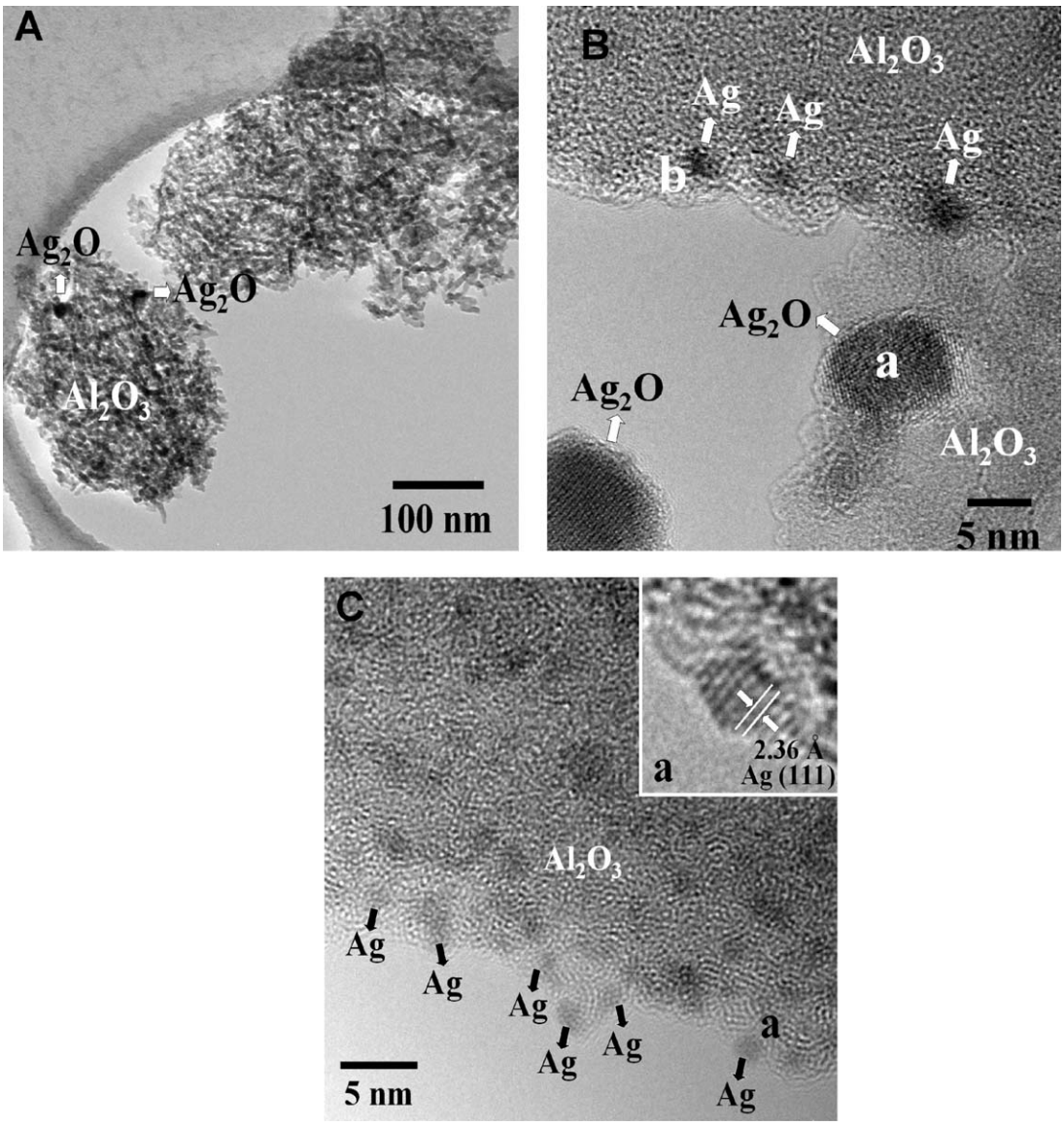

Fig. 4. HRTEM images of fresh (A and B) and aged (C) Al5Ag.

10–20 nm size range). It is interesting to note that metallic Ag crystallites are rarely found to be in contact with the CeO_2 support, they are preferentially located on top Ag_2O particles. Taking into account that Ag metal forms only in contact with large Ag_2O particles and it is not found in contact with small Ag_2O particles and CeO_2, it is likely that the transformation $Ag_2O \rightarrow Ag$ during calcination of the sample is retarded in the presence of CeO_2. This is in contrast to what reported previously in a few studies [45,66] where it was argued that the presence of ceria, due to its well known oxygen storage capacity, facilitates removal of oxygen from silver oxide. On the contrary, and in agreement with our findings, Murrel and Carlin [48] reported that ceria is able to maintain silver in a higher oxidation state, in a manner similar to that observed in other noble metals [67]. It is in fact recognized that by doping other VIII group metals onto the surface of an oxide with powerful redox chemistry the establishing of a strong support oxide interaction is likely, with the effect that metals can be found in an oxidized and dispersed state [65]. Different methods of preparation (i.e. coprecipitation and impregnation) and loading could explain the discrepancies observed. The morphology of the small Ag_2O particles gives additional evidence for a strong interaction with the CeO_2 support (Fig. 2A), since there is always a good contact between Ag_2O particles and CeO_2 crystallites. This strong interaction with CeO_2 may hinder the decomposition of small Ag_2O particles into metallic Ag. In accordance to this, larger Ag_2O particles decompose into metallic Ag at the side opposite to the Ag_2O–CeO_2 interface (Fig. 2B). The fact that diffraction data reveal only the presence of metallic Ag, might be due to the low concentration of Ag_2O particles as well as to their small dimension (ca. 5 nm) that escape XRD detection.

After ageing Ce5Ag shows a different microstructure. CeO_2 crystallites have increased their size upon calcination at higher temperature (Fig. 2C), and the catalyst shows again the presence of metallic Ag and Ag_2O. The main effect of calcination is the increasing of the amount of Ag in metallic state; the sample is constituted by core-shell silver particles (Fig. 2D), where the cores are Ag_2O crystallites of about 10–15 nm in size, and the shell is metallic Ag. Ag_2O crystallites are entirely covered by a smooth metallic Ag layer 3–4 nm thick and no evidence for small Ag_2O particles (ca. 5 nm) is found. These core-shell particles may be the result of $Ag_2O \rightarrow Ag$ transformation of large Ag_2O particles (15–20 nm) present in fresh sample. During the ageing process the decomposition of large Ag_2O particles is hindered by diffusion, while small Ag_2O crystallites readily decompose into metallic Ag

and migrate, covering the cores of Ag_2O with a smooth metallic Ag layer originating the structure that is showed in Fig. 2D.

In Zr5Ag and Al5Ag a different behaviour is recognized. The first important difference between ZrO_2, Al_2O_3 and CeO_2-based catalysts is the shape of Ag_2O particle; rounded shape in CeO_2-supported sample and well-faceted in Zr5Ag (Fig. 3A) and in Al5Ag. This may be interpreted in terms of particle–support interaction. The round-shaped Ag_2O particles in the CeO_2-supported catalyst may arise from a strong interaction as discussed earlier, whereas this interaction could be weaker in the ZrO_2-supported sample resulting in well-faceted crystallites. In contrast to the CeO_2-supported sample, in the fresh Zr5Ag catalyst there are no Ag_2O particles larger than 10 nm.

In aged Zr5Ag sample there are no core-shell particles and metallic Ag particles of about 10–12 nm are dominant over Ag_2O. Fig. 3B shows an individual particle with mixed Ag_2O and Ag domains on top a ZrO_2 crystal and Fig. 3C corresponds to a pure Ag crystallite. The lack of core-shell particles in this catalyst and the fact that fresh Zr5Ag does not contain big Ag_2O particles support the idea that a kinetic control operates in the decomposition of Ag_2O under this conditions.

Al_2O_3-based systems are very similar to Zr5Ag. The fresh sample is constituted by two types of crystallites, corresponding to Ag_2O and Ag phases. Ag_2O crystallites are faceted like in Zr5Ag and have sizes of about 10–20 nm (Fig. 4A and B). In contrast, Ag crystallites are less faceted and are much more smaller and their size range is very narrow, between 2 and 3 nm (Fig. 4B). A very important characteristic in the sample is that the number of Ag crystallites is much greater than that of Ag_2O. This is in accordance to XRD data, where no signals due to Ag_2O phase are detected and the signals due to Ag phase are very low and only few peaks are visible. The small amount of Ag_2O phase is insufficient to originate a detectable XRD signal whereas Ag crystallites are too small and escape XRD detection limit.

After ageing at 1023 K the sample is constituted exclusively by Ag crystallites. There is no evidence for the presence of Ag_2O particles. Fig. 4C shows the excellent dispersion of Ag crystallites in the sample calcined at 1023 K. They exhibit a very narrow size distribution centred at 2–3 nm.

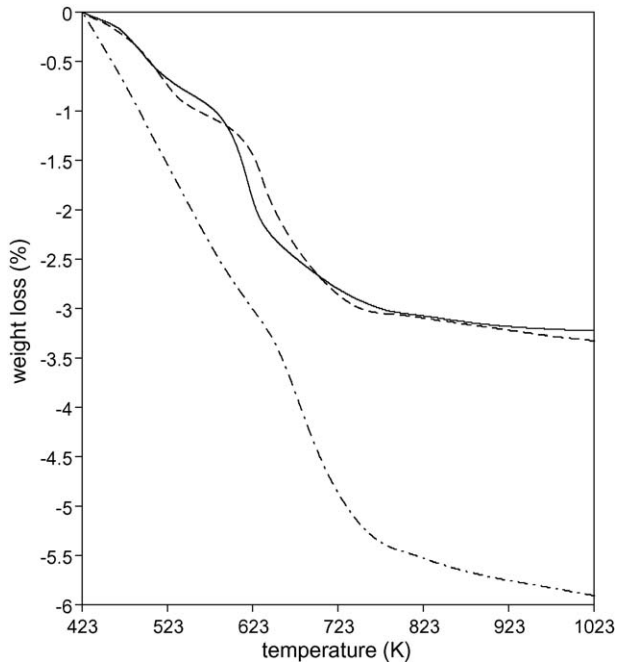

Fig. 5. Weight loss profile obtained by TGA experiments for $AgNO_3/CeO_2$ (solid line), $AgNO_3/ZrO_2$ (broken line) and $AgNO_3/Al_2O_3$ (dotted line).

Table 2
Experimental (TGA results) and theoretical weight loss due to $AgNO_3$ decomposition.

Sample	Theoretical weight loss (100% Ag)[a] (mg)	Theoretical weight loss (20% Ag_2O)[b] (mg)	Experimental weight loss (mg)
Ce1Ag	0.118	0.113	0.138
Ce5Ag	0.570	0.548	0.577
Ce10Ag	1.131	1.087	1.031
Zr5Ag	0.570	0.548	0.586

[a] Assuming that the final mixture contains 100 wt% of Ag.
[b] Assuming that the final mixture contains 20 wt% of Ag_2O.

Summarizing, it is possible to recognize a different behaviour of the silver phase impregnated on ceria compared to zirconia and alumina. On ceria, a strong interaction between the support and the active phase occurs and the transformation $Ag_2O \rightarrow Ag$ is hindered. Moreover, the support influences not only Ag/Ag_2O phase composition but also the shape of crystallites. The CeO_2-based sample is constituted by core-shell particles, where Ag forms a layer on top of Ag_2O. In zirconia and alumina samples, the formation of zero valent Ag is not influenced, the number of Ag particles is much greater than that of Ag_2O (in Al_2O_3 exclusively Ag is formed after ageing) and the crystallites are very well dispersed also after ageing.

Additional insights into the formation of Ag/Ag_2O have been obtained by combined TGA and in-situ XRD. Fig. 5 shows the weight loss profile of samples of Ce5Ag, Zr5Ag and Al5Ag following drying. The onset of decomposition of silver nitrate precursor is at ca. 450 K for both Ce and Zr containing samples and it is completed at around 800 K. The desorption of water does not allow an appropriate quantification of decomposition in the presence of Al_2O_3.

In the case of ceria and zirconia Table 2 compares the weight loss values (experimental vs theoretical) found assuming that all

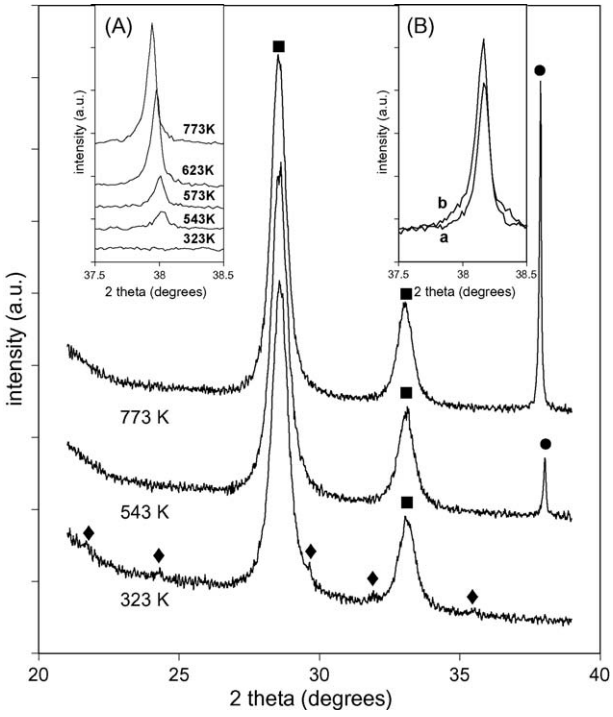

Fig. 6. In-situ XRD profiles during treatment at increasing temperatures in air of $AgNO_3/CeO_2$: CeO_2, ■; Ag, ●; $AgNO_3$, ◆. Detail of the region around $2\theta = 38.1^\circ$ after treatment in air (profile A) and after treatment under H_2/N_2 atmosphere (profile B).

$AgNO_3$ decomposes to metallic Ag according to a two step process:

$$2AgNO_3 \rightarrow Ag_2O + 2NO_2 + 0.5O_2 \quad (1)$$

$$Ag_2O \rightarrow 2Ag + 0.5O_2 \quad (2)$$

The observed weight loss is in agreement with formation of metallic Ag as a final product although the presence of Ag_2O (as confirmed by HRTEM) cannot be distinguished due to the slight weight difference. As an example, assuming the presence of 20 wt% of Ag_2O in the final Ce5Ag the theoretical weight loss would be 0.548 mg which under our conditions cannot be distinguished from the observed values.

Indirect evidence for the formation of Ag_2O in ceria-based system was obtained by following decomposition and subsequent reduction under hydrogen with in-situ XRD. Fig. 6 shows the XRD profile in the region of interest of the starting material subjected to treatment under air at increasing temperatures. At 323 K, peaks attributable to $AgNO_3$ are visible; when the temperature increases it is possible to observe the decomposition of $AgNO_3$ and the associated formation of metallic silver phase (peak at $2\theta = 38.1^\circ$). In insert A the detail of the formation of metallic silver is reported showing that the peak at 38.1° becomes more intense while temperature increases up to ca. 800 K. Insert B shows the XRD profile after calcination in air (profile a) and after treatment in H_2/N_2 atmosphere for 4 h at 473 K (profile b). The increase of the peak intensity is correlated to the reduction of Ag_2O to Ag induced by the reducing atmosphere.

Reducibility of Ag-based catalysts was also characterized by temperature programmed reduction with H_2 (Fig. 7). TPR profile of bare supports (not shown) evidences the typical bimodal shape characteristic of CeO_2 [68] while a flat profile is detected with Al_2O_3 and ZrO_2, in line with their reduction behaviour under TPR conditions [69,70]. The presence of Ag does not modify the TPR traces of ZrO_2 and Al_2O_3. No distinct silver oxide reduction peaks were observed in H_2-TPR which is in agreement with the fact that most of silver is present as zero valent Ag. Ag-modified ceria shows a different behaviour. A broad reduction peak at ca. 380 K is observed in fresh Ce5Ag (Fig. 7A) likely due to reduction of Ag_2O to Ag, since evidence of reduction of ceria at low temperature due to H_2 activation and spillover with Ag/CeO_2 system has not been reported previously [66]. The reduction temperature is consistent with that reported for dispersed Ag_2O on Al_2O_3 [47]. Reduction of Ag_2O in aged Ce5Ag shows a smaller peak centred at ca. 420 K (Fig. 7B); the intensity of the peak indicates that aged Ce5Ag contains less Ag_2O than its fresh counterpart, while the reduction temperature is indicative of a lower dispersion of Ag_2O [47]. The results confirm the HRTEM findings discussed above.

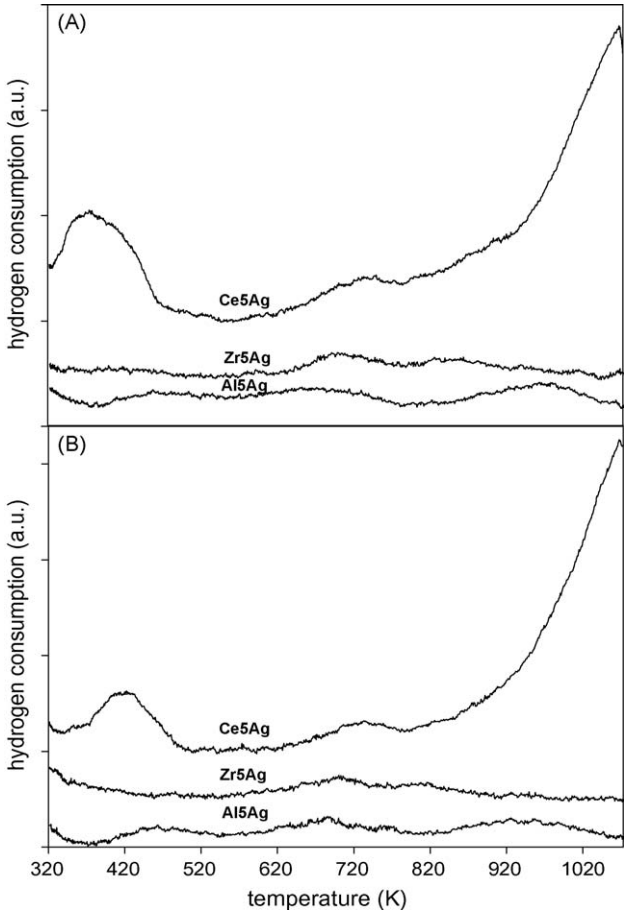

Fig. 7. TPR profile of fresh (A) and aged (B) catalysts.

3.2. Soot combustion

Soot combustion studies were carried out either with a TG apparatus or under TPO conditions in a micro flow reactor. The latter approach was carried out mainly to verify gas composition after combustion, which confirmed the presence of CO_2 only. All the catalysts examined, mixed with soot under tight contact conditions, are active in promoting combustion at temperature below 650 K. As a measure of activity we used the temperature at which 50% of weight loss is observed. The lower oxidation temperatures were found between 5% and 10% loading (Fig. 8). The former loading was then selected for additional studies. The results for all supports at this loading are reported in Fig. 9. In all samples investigated a remarkable decrease of oxidation temperature is achieved by adding silver; this is higher for Al_2O_3 and ZrO_2 supports (the best results are obtained with fresh Zr5Ag in which a T_{50} of 606 K was found, Fig. 9A) and lower for CeO_2, which shows the highest activity as a bare support. Also, the onset temperature for combustion is lowered to ca. 500 K by adding silver. A comparison with other catalysts shows that silver-doped materials can be included among the most promising systems investigated

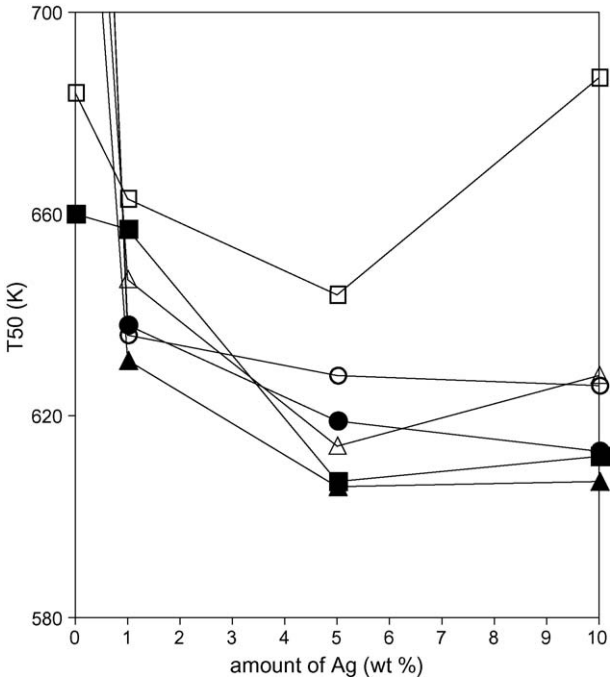

Fig. 8. Effect of Ag loading on T_{50} for fresh (filled symbols) and aged (open symbols) catalysts: CeO_2, ■; ZrO_2, ▲; Al_2O_3, ● (for pure zirconia and alumina see Fig. 9).

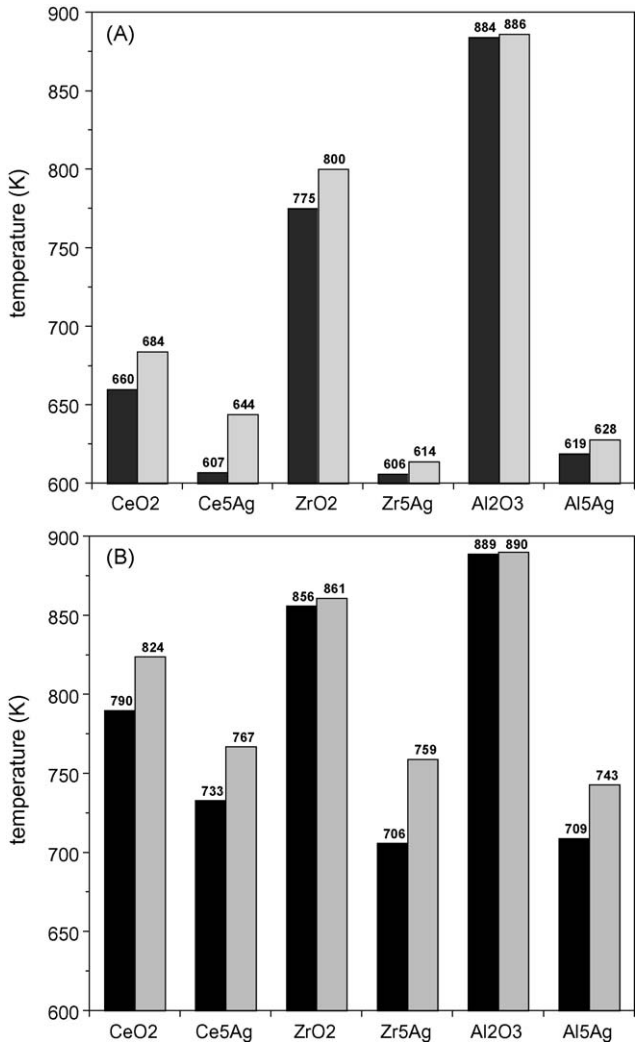

Fig. 9. T_{50} as measured in soot combustion for both fresh (dark bars) and aged (light bars) catalysts, in tight contact (A) and loose contact (B) conditions.

(Table 3). Fig. 9B shows the results under loose contact conditions. For all samples, the T_{50} under loose contact is higher than under tight contact, due to a less efficient type of contact between soot and catalyst. The activity of silver-based catalyst always showed an improvement compared to bare supports, with Zr5Ag and Al5Ag showing a combustion temperature of ca. 100 K lower than the individual supports.

While it is clear that the presence of silver is the main factor contributing to the overall activity the presence of the support does also affect the activity of the catalyst under both tight and loose contact conditions. In the first case the addition of Ag is particularly beneficial to Al_2O_3 and ZrO_2 where a decrease of more than 250 K (170 K for ZrO_2) in the T_{50} is observed either with material under fresh or under aged conditions. With ceria a decrease of ca. 50 K (and 40 K for the aged catalyst) is observed. This behaviour is likely due to a different interaction between silver and the support which affects the transformation $Ag_2O \rightarrow Ag$ during preparation/calcination. In particular zirconia and alumina seem to benefit from the larger quantities of metallic Ag, while in the presence of ceria the larger amount of Ag_2O coupled with the higher initial activity of the bare support reduces the overall effect of silver. In addition, the dispersion of Ag is also affected by the support, being higher over alumina and zirconia and lower with ceria where Ag forms a smooth metallic layer on top of Ag_2O. These effects are also evidenced measuring activity under loose conditions where for both fresh and aged catalysts the activity of Ag on ZrO_2 and Al_2O_3 is higher than that of Ag on CeO_2.

In order to better understand the role of Ag particles in soot oxidation we treated our samples under reducing atmosphere (5%H_2/Ar) for 2 h at 473 K to complete the transformation of any residual Ag_2O to Ag. Catalytic results on reduced catalysts are shown in Fig. 10. An important difference in T_{50} is observed only for Ce5Ag (which shows the lowest T_{50} among all the samples tested) indicating that CeO_2-based catalyst is the only one that retarded the Ag_2O/Ag transformation in agreement with HRTEM results. Indeed, in Zr- and Al-supported samples, where almost all the silver is in the metallic state, the reduction in H_2/Ar atmosphere does not influence the activity. One could conclude that ceria maintains silver in an oxidation state at the ceria surface which is not ideal for assisting the soot oxidation reaction; whereas when silver itself is reduced to the zero valent state a more potent soot combustion catalyst is formed. It is in fact well know that metallic silver is an oxidation catalyst that can form several suboxide

Table 3
Activity of different catalyst formulations.

Catalyst	T_{OX}[a] (K)	Temp. calc. (K)	Ratio soot/catalyst	% O_2	Ref.
$K_{2x}Cu_{1-x}Fe_2O_4$; $K_xLa_{1-x}FeO_3$	~573	923, 3 h	1:9	n.a.	[16]
$Cs_4V_2O_7$	574	973, 2 h	2:1	20	[9]
$KCuV/Al_2O_3$	583	973, 4 h	1:20	20	[15]
$Cs_4V_2O_7/Al_2O_3$	587	973, 2 h	2:1	20	[9]
Co/CeO_2	573–613	673	1:20	6	[34]
Ag/ZrO_2	614	1023, 12 h	1:20	20	This work
Co, K/CeO_2	623	673	1:20	6	[10]
Cu-K-Mo/TiO_2 o ZrO_2	651	773	1:2	21	[13]
Cu-K-V-Cl/TiO_2	655	973, 12 h	1:10	10	[8]
Cu-K-Mo-Cl/TiO_2	663	873	1:9	21	[17]
K/CeO_2; Ba, K/CeO_2; K/La_2O_3	623–673	673	1:20	6	[11]
Co, K/MgO	~673	673	1:20	6	[18]
$Cu_{1.96}K_{3.45}/ZrO_2$	678	873, 4 h	1:16	21	[35]
CeO_2-5La	683	1273, 1.5 h	1:4	21	[27]
Ag/Mn	681	773	1:2	21	[13]
KOH/MgO	713	1037, 0.5 h	1:4	21	[19]
Ba/CeO_2	753	673	1:20	6	[11]
$LaCrO_3$; $LaCr_{0.9}O_3$; $LaCr_{0.8}O_3$; $LaVCr_{0.9}O_3$	723–773	n.a.	1:9	20	[20]
Co/MgO	>773	973	1:20	6	[18]
LaMnBO; $LaFeO_3$; $LaMnO_3$; $La_{1-x}K_xMnO_3$	773–823	n.a.	1:9	20	[20]

[a] Oxidation temperature of soot measured either with temperature programmed combustion or with thermogravimetric methods.

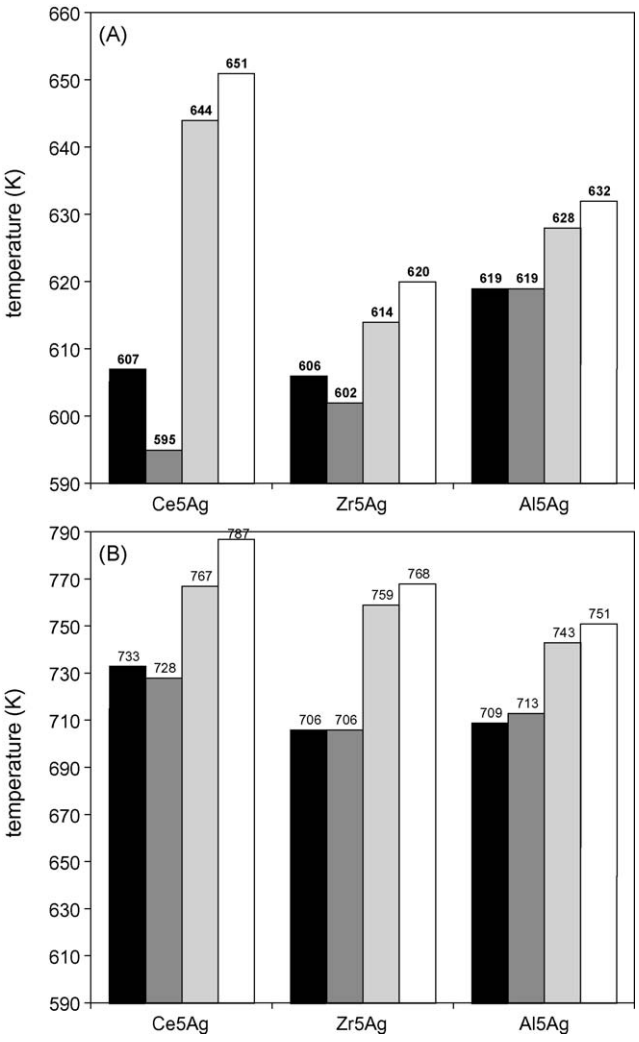

Fig. 10. TGA results (T_{50}) for soot combustion for fresh samples (dark bars), samples reduced in H_2/Ar (dark grey bars), aged samples (light grey bars) and samples subjected to hydrothermal treatment (light bars) in tight contact (A) and in loose contact (B).

species in oxidation atmosphere [40,41,46,71–73] and can also promote the formation of superoxide O^{2-} ions [36] that might assist carbon oxidation. However, the decrease of activity after ageing observed in Ce5Ag is higher than that observed on the other supports despite the fact that the amount of metallic silver increases. This can be explained by the lower thermal stability of ceria-based materials (surface area of the aged sample is 13 m^2/g) and to the different silver dispersion. Core-shell particles, as detected by HRTEM, are likely to decrease Ag dispersion in ceria, while smaller Ag particles are observed with alumina and zirconia.

Fig. 10 shows also the effect of ageing under hydrothermal conditions following calcination at 1023 K in the presence of water. All samples maintain their activity and no dramatic decrease in performance are observed with ZrO_2 and Al_2O_3-based catalysts performing better than Ag/ceria. This is likely due to the lower thermal stability of ceria under these conditions [65].

4. Conclusion

A combination of TGA, TPR experiments and HRTEM characterization shows that catalyst formulations containing silver are active for soot oxidation over the supports investigated. Formation of Ag/Ag_2O mixture is observed in all supports and their relative abundance is strictly correlated to the nature of the support. Ceria is shown to stabilize silver in the oxide state, while with ZrO_2 and Al_2O_3 metallic Ag is preferentially formed. For this reason addition of Ag to ZrO_2 and Al_2O_3 results in very active catalysts in a fresh or aged state while in the case of ceria the addition of silver has little benefit. This is due either to a different distribution of Ag/Ag_2O particles and to the fact that ceria itself is active in soot oxidation. It is likely that the mechanism of action of ceria and silver are different, the former being related to the redox action of ceria and to its ability to deliver oxygen from the lattice/surface to the soot particle in a wide temperature range [22–24], the latter being correlated to the formation of several suboxide species and superoxide O^{2-} ions that might assist carbon oxidation as proposed for CO and methane oxidation over supported silver catalysts [40,46].

Acknowledgments

The authors thank financial support from MIUR (progetti PRIN) and MEC (ENE2006-06925). We are also grateful to Grace Davison (USA) for providing starting materials used in this study.

References

[1] B.A.A.L. van Setten, M. Makkee, J.A. Moulijn, Catal. Rev. Sci. Eng. 43 (2001) 489.
[2] D. Fino, Sci. Technol. Adv. Mat. 8 (2007) 93.
[3] M. Twigg, Appl. Catal. B 70 (2007) 2.
[4] M. Shelef, R.W. McCabe, Catal. Today 62 (2000) 35.
[5] P. Zelenka, W. Cartellieri, P. Herzog, Appl. Catal. B 10 (1996) 3.
[6] G.A. Stratakis, A.M. Stamatelos, Combust. Flame 132 (2003) 157.
[7] B.A.A.L. van Setten, J.M. Schouten, M. Makkee, J.A. Moulijin, Appl. Catal. B 28 (2000) 253.
[8] P. Ciambelli, V. Palma, P. Russo, S. Vaccaro, J. Mol. Catal. A 204–205 (2003) 673.
[9] G. Saracco, C. Badini, N. Russo, V. Specchia, Appl. Catal. B 21 (1999) 233.
[10] E.E. Miro', F. Ravelli, M.A. Ulla, L.M. Cornaglia, C.A. Querini, Catal. Today 53 (1999) 631.
[11] M.L. Pisarello, V. Milt, M.A. Peralta, C.A. Querini, E.E. Mirò, Catal. Today 75 (2002) 465.
[12] V.G. Milt, C.A. Querini, E.E. Miro', M.A. Ulla, J. Catal. 220 (2003) 424.
[13] J.P.A. Neeft, M. Makkee, J.A. Moulijn, Appl. Catal. B 8 (1996) 57.
[14] P. Ciambelli, V. Palma, P. Russo, S. Vaccaro, Catal. Today 73 (2002) 363.
[15] G. Neri, G. Rizzo, S. Galvagno, M.G. Musolino, A. Donato, R. Pietropaolo, Therm. Acta 381 (2002) 165.
[16] H. An, C. Kilroy, P.J. McGinn, Catal. Today 98 (2004) 423.
[17] C. Badini, G. Saracco, V. Serra, V. Specchia, Appl. Catal. B 18 (1998) 137.
[18] C.A. Querini, M.A. Ulla, F. Requejo, J. Soria, U.A. Sedrán, E.E. Mirò, Appl. Catal. B 15 (1998) 5.
[19] R. Jimenez, X. Garcia, C. Cellier, P. Ruiz, A.L. Gordon, Appl. Catal. A 297 (2006) 125.
[20] D. Fino, P. Fino, G. Saracco, V. Specchia, Korean J. Chem. Eng. 20 (2003) 445.
[21] M. Makkee, S.J. Jelles, J.A. Moulijin, in: A. Trovarelli (Ed.), Catalysis by Ceria and Related Materials, Imperial College Press, 2002, p. 391.
[22] E. Aneggi, M. Boaro, C. de Leitenburg, G. Dolcetti, A. Trovarelli, Catal. Today 112 (2006) 94.
[23] E. Aneggi, M. Boaro, C. de Leitenburg, G. Dolcetti, A. Trovarelli, J. Alloys Compd. 408–412 (2006) 1096.
[24] E. Aneggi, C. de Leitenburg, G. Dolcetti, A. Trovarelli, Catal. Today 114 (2006) 40.
[25] E. Aneggi, C. de Leitenburg, G. Dolcetti, A. Trovarelli, Catal. Today 136 (2008) 3.
[26] E. Aneggi, C. de Leitenburg, G. Dolcetti, A. Trovarelli, Top. Catal. 42–43 (2007) 319.
[27] A. Bueno-López, K. Krishna, M. Makkee, J.A. Moulijin, J. Catal. 230 (2005) 237.
[28] M.A. Peralta, V.G. Milt, L.M. Cornaglia, C.A. Querini, J. Catal. 242 (2006) 118.
[29] K. Krishna, A. Bueno-López, M. Makkee, J.A. Moulijn, Appl. Catal. B 75 (2007) 189.
[30] K. Krishna, A. Bueno-López, M. Makkee, J.A. Moulijn, Appl. Catal. B 75 (2007) 201.
[31] K. Krishna, A. Bueno-López, M. Makkee, J.A. Moulijn, Appl. Catal. B 75 (2007) 210.
[32] L. Zhu, J. Yu, X. Wang, J. Hazard. Mater. 140 (2007) 205.
[33] X. Wu, D. Liu, K. Li, J. Li, D. Weng, Catal. Commun. 8 (2007) 1274.
[34] P.G. Harrison, I.K. Ball, W. Daniell, P. Lukinskas, M. Caspedes, E.E. Mirò, M.A. Ulla, Chem. Eng. J. 95 (2003) 47.
[35] H. Laversin, D. Courcot, E.A. Zhilinskaya, R. Cousin, A. Aboukaïs, J. Catal. 241 (2006) 456.
[36] M. Machida, Y. Murata, K. Kishikawa, D. Zhang, K. Ikeue, Chem. Mater. 20 (2008) 4489.
[37] Y. Shiraishi, N. Toshima, J. Mol. Catal. A 141 (1999) 187.
[38] C.F. Mao, M.A. Vannice, Appl. Catal. A 122 (1995) 61.
[39] A.N. Pestryakov, Catal. Today 28 (1996) 239.
[40] Lj. Kundakovic, M. Flytzani-Stephanopoulos, Appl. Catal. A 183 (1999) 35.
[41] A. Nagy, G. Mestl, Appl. Catal. A 188 (1999) 337.
[42] P.W. Park, C.L. Boyer, Appl. Catal. B 59 (2005) 27.
[43] R. Brosius, K. Arve, M.H. Groothaert, J.A. Martens, J. Catal. 231 (2005) 344.

[44] L. Gang, B.G. Anderson, J. van Grondelle, R.A. van Santen, W.J.H. van Gennip, J.W. Niemantsverdriet, P.J. Kooyman, A. Knoester, H.H. Brongersma, J. Catal. 206 (2002) 60.
[45] S. Imamura, H. Yamada, K. Utani, Appl. Catal. A 192 (2000) 221.
[46] Z. Qu, M. Cheng, W. Huang, X. Bao, J. Catal. 229 (2005) 446.
[47] M. Luo, X. Yuan, X. Zheng, Appl. Catal. A 175 (1998) 121.
[48] L.L. Murrel, R.T. Carlin, J. Catal. 159 (1996) 479.
[49] K. Villani, R. Brosius, J.A. Martens, J. Catal. 236 (2005) 172.
[50] J.F. Lamonier, N. Sergent, J. Matta, A. Aboukaïs, J. Therm. Anal. Calorim. 66 (2001) 645.
[51] B.R. Stanmore, J.F. Brilhac, P. Gilot, Carbon 39 (2001) 2247.
[52] S.J. Jelles, B.A.A.L. Van Setten, M. Makkee, J.A. Moulijn, Appl. Catal. B 21 (1999) 35.
[53] G. Mul, F. Kapteijin, J.A. Moulijn, Appl. Catal. B 12 (1997) 33.
[54] Z. Sarbak, K. Surma, J. Therm. Anal. Calorim. 72 (2003) 159.
[55] A. Carrascull, C. Grzona, D. Lick, M. Ponzi, E. Ponzi, React. Kinet. Catal. Lett. 75 (2002) 63.
[56] J.P.A. Neeft, M. Makkee, J.A. Moulijn, Chem. Eng. J. 64 (1996) 292.
[57] J.P.A. Neeft, O.P. van Pruissen, M. Makkee, J.A. Moulijn, Appl. Catal. B 12 (1997) 21.
[58] V.G. Milt, M.L. Pisarello, E.E. Mirò, C.A. Querini, Appl. Catal. B 41 (2003) 397.
[59] V. Serra, G. Saracco, C. Badini, V. Specchia, Appl. Catal. B 11 (1997) 329.
[60] R.J. Farrauto, R.M. Heck, Catal. Today 51 (1999) 351.
[61] J.C. Summers, S.V. Houtte, D. Psaras, Appl. Catal. B 10 (1996) 139.
[62] V.G. Milt, C.A. Querini, E.E. Mirò, Thermochim. Acta 404 (2003) 177.
[63] G. Morterra, G. Magnacca, V. Bolis, G. Cerrato, M. Baricco, A. Giachello, M. Fucale, Stud. Surf. Sci. Catal. 96 (1995) 361.
[64] A. Piras, A. Trovarelli, G. Dolcetti, Appl. Catal. B 28 (2000) L77.
[65] A. Trovarelli, Catal. Rev. Sci. Eng. 38 (1996) 439.
[66] L. Kundakovic, M. Flytzani-Stephanopoulos, J. Catal. 179 (1998) 203.
[67] L.L. Murrel, S.J. Tauster, D.R. Anderson, Catalysis and Automotive Pollution Control II, Elsevier, Amsterdam, 1991, p. 547.
[68] F. Giordano, A. Trovarelli, C. de Leitenburg, M. Giona, J. Catal. 193 (2000) 273.
[69] E.P. Reddy, R.S. Varma, J. Catal. 221 (2004) 93.
[70] L. Ilieva, J.W. Sobczak, M. Manzoli, B.L. Su, D. Andreeva, Appl. Catal. A 291 (2005) 85.
[71] N. Gungor, S. Isci, E. Gunister, W. Mista, H. Teterycz, R. Klimkiewicz, Appl. Clay Sci. 32 (2006) 291.
[72] Z. Qu, M. Cheng, X. Dong, X. Bao, Catal. Today 93–95 (2004) 247.
[73] G.I.N. Waterhouse, G.A. Bowmaker, J.B. Metson, Appl. Surf. Sci. 214 (2003) 36.